Analyzing-power measurements in the $^3H(\vec{p}, n)^3He$ reaction*

J. J. Jarmer,† R. C. Haight,‡ J. E. Simmons, and J. C. Martin
Los Alamos Scientific Laboratory, University of California, Los Alamos, New Mexico 87544

and

T. R. Donoghue§
Los Alamos Scientific Laboratory, University of California, Los Alamos, New Mexico 87544, and The Ohio State University, Columbus, Ohio 43210

(Received 31 December 1973)

Angular distributions of the analyzing power of the reaction $^3H(\vec{p},n)^3He$ have been measured at proton energies of 6.00, 9.96, and 13.55 MeV. These data are compared with available neutron-polarization data for the same reaction on a point-by-point basis and by means of associated Legendre-polynomial coefficients. In contrast to the comparison below 4 MeV, no significant difference exists above 6 MeV between the two observables at the same energies and angles. The data are also compared with R-matrix calculations based on the parameter sets of Werntz and Meyerhof. The previously reported excitation function for the analyzing power at $\theta_{c.m.} = 45°$ from 1.5 to 12 MeV is further documented.

[NUCLEAR REACTIONS $^3H(\vec{p},n)^3He$, $E = 6.00$, 9.96, and 13.55 MeV; measured analyzing power $A(\theta)$.]

I. INTRODUCTION

In a previous letter[1] we reported on measurements of the analyzing power A (45° c.m.) for the reaction $^3H(\vec{p}, n)^3He$ as a function of incident proton energy E_p. These measurements were compared with existing polarization data P (45° c.m.) for the reaction because considerations based on charge symmetry of nuclear forces and on time reversal indicate that P and A should be approximately equal at a given energy and angle. The preceding assumes that Q-value and charge-dependent effects can be ignored. The result of the experimental comparison was that P and A at 45° c.m. had similar excitation functions but that the magnitude of P was generally less than that of A, an effect that was most pronounced between $E_p = 1.7$ and 4 MeV. The data were also compared with calculations based on the levels of ^4He from the charge-independent R-matrix analysis of the reaction $^3H(p, n)^3He$ by Werntz and Meyerhof[2] (hereafter denoted as WM). The shapes of the excitation functions for both P and A were reproduced by these calculations but the magnitudes were not. Furthermore, the calculations predicted that P and A should be approximately equal, in disagreement with experiment but consistent with the symmetries mentioned above. Recently, our experimental results for A (45° c.m.) have been corroborated by Brown and Rohrer[3] for E_p < 3 MeV.

In the present work, angular distributions of the analyzing power $A(\theta)$ have been measured for proton energies of 6.00, 9.96, and 13.55 MeV. Our object was to provide further precise data concerning the four-nucleon system and to pursue the comparison between P and A. These comparisons are facilitated by the existence of $^3H(p, n)^3He$ differential cross-section data[4] which were used in associated Legendre-polynomial expansions of $P(\theta)[d\sigma(\theta)/d\Omega]$ and $A(\theta)[d\sigma(\theta)/d\Omega]$. For reference purposes the previously reported analyzing-power measurements at 45° c.m. are presented in tabular form.

II. EXPERIMENTAL METHOD

The analyzing power was determined by initiating the reaction with a transversely polarized proton beam and measuring the asymmetry of the neutrons produced with the incident-beam polarized parallel (+) or antiparallel (−) to the normal vector to the reaction plane, $\vec{n} \propto \vec{k}_{in} \times \vec{k}_{out}$. The dc-polarized proton beam was produced by the Los Alamos Lamb-shift polarized-ion source[5] and accelerated by an FN tandem Van de Graaff. The beam was polarized vertically by spin precession before injection into the accelerator. Reversal of the spin direction on target was accomplished by reversing fields in the ion source as explained in Ref. 5. The magnitude of the proton polarization was typically about 0.90 and was measured

by an atomic-beam technique[6] to an accuracy of ±0.015. The accelerated beam was directed onto a cylindrical (3-cm-long by 0.8-cm-diam) stainless-steel gas cell containing gaseous tritium at 2.6 or 4.7 atm absolute. The entrance foil to the target was either a 9.8-mg/cm^2 molybdenum foil plated with 2.4-mg/cm^2 nickel or a 2.1-mg/cm^2 Havar[7] foil. The lower gas pressure and the Havar foil were used for the measurements at 6 MeV while the higher pressure and molybdenum-nickel foil were used for those at 9.96 and 13.55 MeV. The contributions to the proton energy spread at 9.96 MeV due to straggling in the Mo-Ni foil and the energy loss through half the gas cell were 0.074 and 0.059 MeV, respectively. At 13.55 MeV the values are 0.071 and 0.045 MeV. At 6.00 MeV the straggling in the Havar foil and the energy loss through half the gas cell were 0.030 and 0.051 MeV.

The beam was stopped by 0.48 mm of gold which also served as the end wall of the tritium cell. The gas-target assembly was electrically insulated from the rest of the beam line and served as a Faraday cup. Secondary electrons were suppressed by maintaing an insulated section of the beam line immediately before the target at a potential of −300 V. The beam current on the target was monitored by a current integrator so that each + and − run of an asymmetry measurement could be normalized to the same integrated beam current. The stability of the current integrator proved to be better than 0.3% over a period of 1.5 h.

Neutrons produced from the reaction $^3H(p, n)^3He$ were detected by a cylindrical (4.4-cm-diam by 4.4-cm in length) NE-213 scintillator. The scintillator was positioned directly behind and on the centerline of the bore of a spin-precession solenoid which, for these measurements, was turned off and served only as a collimator. The distance from the tritium cell center to the scintillator center was 85 cm. At this distance the scintillator subtended an angle (full width) of $\Delta\theta = 3°$. Our results are not corrected for finite geometry. A neutron-beam profile measurement was taken at 13.55 MeV to determine the true zero of angle. Neutrons were separated electronically from γ rays using pulse-shape discrimination. Figure 1 shows a typical time spectrum obtained from the time-to-amplitude converter (TAC) of the pulse-shape discrimination system. To estimate how well the γ rays were rejected, several n-γ rejection ratios were calculated. The rejection ratio was obtained by extrapolating the γ-ray peak under the neutron peak in the time distribution and taking the ratio of their areas. The TAC spectrum shown in Fig. 1 gave the smallest ratio calculated which was 216:1.

The pulse-height information of the proton recoils was split and fed, on one side, to single-channel analyzers which drove fast scalers, and on the other, to an analog-to-digitial converter (ADC). The multichannel spectrum from the latter was stored in an XDS-930 computer.

Dead time in the electronics was potentially important in the TAC used in the n-γ discrimination. Counting rates at the start input of the TAC were kept low so that the dead time was always less than 0.7%. The corrections to A were estimated to be always less than 0.0006 and hence, were neglected. No dead-time correction was required for either the single-channel analyzers or the scalers.

III. DATA ACQUISITION AND REDUCTION

The analyzing power was calculated from the expression

$$A = \frac{N_+ - N_-}{p_- N_+ + p_+ N_-}, \tag{1}$$

where N is the number of neutrons detected with the incident-proton-beam polarized parallel (+) or antiparallel (−) to the normal to the reaction plane; p_+ and p_- are the beam polarizations for the two orientations. In order to reduce the effect of electronic drifts, the data were taken in two cycles of + − − + beam polarization. Each + and − run within a cycle was short; a run typically lasted two minutes. The beam polarization was measured after each + or − run in a cycle.

The recoil proton distribution exhibited the well-known shape for elastic low-energy n-p scattering and served as a diagnostic check on system

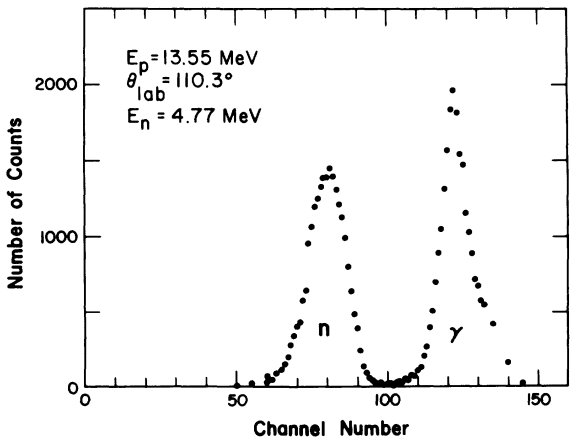

FIG. 1. Typical time spectrum obtained from the time-to-amplitude converter of the n-γ discrimination system.

operation. In cases where the shape of the recoil distribution indicated that background neutrons were not negligible, target-empty runs were taken. The target-empty runs indicated that the majority of the background neutrons were produced in the metal of the target, collimating slits, etc. The target-empty runs were taken in the same + − − + sequence as target-full runs and for the same integrated beam current. It was observed that at each proton energy the background was approximately isotropic. In particular, the background exhibited no asymmetry when the beam polarization was reversed from + to −. The background was most serious for the backward angles (>90° lab) where the neutron energy is lower. We also observed that the background decreased with decreasing proton energy.

Asymmetries were obtained during a run by setting two single-channel analyzer windows on the recoil-proton distribution. These windows were designated as the lower window and upper window. The lower cutoffs of the lower and upper windows were typically 50 and 75%, respectively, of the recoil one-half point of the distribution. The recoil one-half point is defined as the pulse height at the high-energy end of the distribution where the number of counts per channel decreases to one half of the counts per channel in the flat part of the distribution. The upper cutoff was the same for both windows and was set high enough to include the entire rounded edge at the high-energy end of the distribution. After each + and − sequence in a cycle, an asymmetry was calculated for each window. These asymmetries were compared and served as a running check on possible electronic drifts, background, etc.

To indicate the quality of the experimental data, Fig. 2 shows four typical recoil-proton distributions. In all the distributions the lower cutoff was set high enough in the electronics to eliminate excessive counts from noise. The low-energy tail is due to target-empty neutrons and some γ rays. The arrows labeled L and U indicate the lower levels of the lower and upper windows chosen to calculate the analyzing power. The unlabeled arrow indicates the common upper cutoff. Figure 2(a) shows the recoil-proton distribution obtained at 45.3° lab for a proton energy of 13.55 MeV. At this angle the energy of the neutrons from the reaction is well above the energy of the target-empty neutrons; consequently the latter are not a problem. Figure 2(b) shows the distribution at 110.3° lab for a proton energy of 13.55 MeV. Also plotted in this figure are the target-empty distribution and the distribution that results when target empty is subtracted from target full. At this angle the energy of the neutrons from the reaction is lower, and as a result, the contributions of the target-empty neutrons to the total spectrum are not negligible. By subtracting the target-empty from the target-full distribution, however, one obtains a spectrum with the expected shape. This subtraction does not remove low-energy neutrons from proton-induced breakup of the tritium or room-scattered neutrons; we believe that these sources of background are small. Figures 2(c) and 2(d) show the distributions measured at 45.3 and 110.3°, respectively, for a proton energy of 6 MeV. Also plotted in Fig. 2(d) is a very small target-empty contribution.

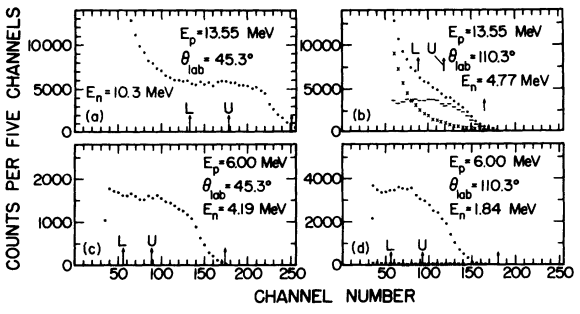

FIG. 2. Typical proton-recoil spectra. Dots are target-full spectra; crosses are target empty; horizontal bars are target full minus target empty.

After a run was completed, the data were further processed with the aid of an off-line computer program. In particular the deduced asymmetries were verified to be independent of whichever portion of the proton recoil spectrum was used. In order to reduce the effect of background neutrons, the analyzing powers calculated from the upper windows have been put in the data tables.

Repeat measurements of five different data points were taken. Each measurement repeated within the statistical error which was typically ±0.003. The errors in the analyzing power were taken as the statistical error expressed as standard deviation and do not contain a contribution from an uncertainty in the beam polarization (±0.015 absolutely, or ±1.7%) which is regarded as being better represented as a systematic error.

To obtain an estimate of other systematic errors, measurements were performed at 0.3° lab, for proton energies of 13.55 and 6.00 MeV. The results were extrapolated to 0° where the analyzing power is zero. The extrapolated results were 0.0023 ± 0.0026 and − 0.0048 ± 0.0023. The weighted average of the absolute values of the extrapolated results is 0.0037 and from this the systematic error in A, not including the uncertainty in beam polarization, is estimated to be less than 0.005.

TABLE I. Angular distribution of the $^3H(\vec{p},n)^3He$ analyzing power.

θ_{lab} (deg)	$\theta_{c.m.}$ (deg)	$A \pm \Delta A$ [a]
	$E_p = 6.00$ [b] ± 0.06 [c] MeV	
0.3	0.4	-0.0062 ± 0.0023
7.8	10.6	-0.0418 ± 0.0024
15.3	20.8	-0.0726 ± 0.0025
22.8	30.9	-0.1054 ± 0.0020
33.5	45.2	-0.1426 ± 0.0023
37.8	50.8	-0.1513 ± 0.0025
45.3	60.4	-0.1496 ± 0.0026
52.8	69.8	-0.1281 ± 0.0032
60.3	78.9	-0.0774 ± 0.0032
70.3	90.5	0.0532 ± 0.0035
80.3	101.5	0.1791 ± 0.0033
90.3	111.8	0.2140 ± 0.0028
100.3	121.5	0.1849 ± 0.0029
110.3	130.4	0.1375 ± 0.0027
120.3	138.8	0.0983 ± 0.0026
130.3	146.6	0.0738 ± 0.0025
	$E_p = 9.96 \pm 0.09$ MeV	
7.8	10.5	-0.0673 ± 0.0026
15.3	20.6	-0.1430 ± 0.0027
22.8	30.6	-0.2110 ± 0.0025
30.3	40.6	-0.2580 ± 0.0027
37.8	50.3	-0.2706 ± 0.0030
45.3	59.8	-0.2415 ± 0.0028
52.8	69.2	-0.2026 ± 0.0030
60.3	78.2	-0.1566 ± 0.0030
70.3	89.7	-0.1008 ± 0.0033
80.3	100.7	-0.0181 ± 0.0040
90.3	111.0	0.0880 ± 0.0040
100.3 [d]	121.0	0.1534 ± 0.0038
110.3	130.0	0.1577 ± 0.0046
120.3	138.1	0.1083 ± 0.0036
130.3	146.0	0.0772 ± 0.0031
80.3 [d]	100.7	-0.0157 ± 0.0037
90.3 [d]	111.0	0.0875 ± 0.0022
	$E_p = 13.55 \pm 0.08$ MeV	
0.4	0.5	-0.0047 ± 0.0026
7.8	10.5	-0.0467 ± 0.0020
15.3	20.6	-0.0988 ± 0.0022
22.8	30.5	-0.1658 ± 0.0021
30.3	40.4	-0.2366 ± 0.0025
37.8	50.1	-0.2821 ± 0.0030
45.3	59.6	-0.2484 ± 0.0028
52.8	68.9	-0.2122 ± 0.0032
60.3	77.9	-0.1500 ± 0.0035
70.3	89.5	-0.1105 ± 0.0031
80.3	100.4	-0.0517 ± 0.0035
90.3	110.7	0.0196 ± 0.0042
100.3	120.4	0.1158 ± 0.0050
110.3	129.4	0.1568 ± 0.0055
120.3	137.8	0.1270 ± 0.0058

[a] Errors are statistical standard deviations.
[b] E_p is proton laboratory energy at target center.
[c] ΔE_p is the sum (in quadrature) of the half-width at half maximum of the theoretical straggling in the entrance foil to the gas cell plus half of the proton energy loss as it passes through the gas.
[d] $E_p = 10.00 \pm 0.04$ MeV.

IV. RESULTS AND DISCUSSION

A. Tabulation of data

The experimental values of the analyzing power are given in Table I. The errors are statistical and are expressed as standard deviations. Systematic uncertainties including that of the beam polarization are not included. In Table II we document the data of our prior communication[1] on A at 45° c.m. as a function of energy. For these data the laboratory angle was near 33° and we observed that the direct $^3H(p, n)^3He$ neutrons were well above the background neutrons; consequently, target-empty runs were not required. For proton energies below 3 MeV the analyzing power changes rapidly with energy; here the tritium gas pressure in the target was reduced to 0.8 absolute atm for most of the measurements. Below 3 MeV the contributions to proton energy spread due to straggling in the Havar foil and energy loss through half the gas cell were typically 0.03 and 0.04 MeV, respectively.

TABLE II. $^3H(\vec{p},n)^3He$ analyzing power near 45° c.m.

E_p [a] $\pm \Delta E_p$ [b] (MeV)	$\theta_{c.m.}$ (deg)	$A_y \pm \Delta A_y$ [c]
1.51 ± 0.06	46.7	0.1810 ± 0.0055
1.67 ± 0.06	45.9	0.2983 ± 0.0053
1.76 ± 0.14	45.6	0.3515 ± 0.0052
1.85 ± 0.05	45.1	0.3983 ± 0.0040
1.92 ± 0.05	45.4	0.4340 ± 0.0041
2.01 ± 0.05	45.1	0.4616 ± 0.0040
2.13 ± 0.05	45.3	0.4804 ± 0.0045
2.26 ± 0.05	45.2	0.4701 ± 0.0039
2.51 ± 0.11	45.3	0.4156 ± 0.0031
2.76 ± 0.10	45.2	0.3454 ± 0.0025
3.00 ± 0.10	45.4	0.2807 ± 0.0026
3.50 ± 0.08	45.3	0.1848 ± 0.0035
4.00 ± 0.08	45.3	0.1032 ± 0.0025
4.92 ± 0.13	45.4	-0.0245 ± 0.0022
5.94 ± 0.12	45.3	-0.1391 ± 0.0024
6.94 ± 0.11	45.4	-0.2069 ± 0.0023
7.94 ± 0.10	45.4	-0.2394 ± 0.0022
8.50 ± 0.10	45.4	-0.2563 ± 0.0021
8.95 ± 0.10	45.4	-0.2636 ± 0.0020
9.45 ± 0.10	45.5	-0.2652 ± 0.0045
10.46 ± 0.09	45.4	-0.2865 ± 0.0052
10.96 ± 0.09	45.4	-0.2874 ± 0.0046
11.46 ± 0.09	45.4	-0.2735 ± 0.0043
11.95 ± 0.09	45.3	-0.2699 ± 0.0042

[a] E_p is laboratory energy at target center.
[b] ΔE_p is defined as in Table I.
[c] Errors are statistical standard deviations.

TABLE III. Coefficients in the associated Legendre-polynomial expansions Eqs. (2) and (3).

E_p (lab) (MeV)	Quantity	$l_{max}=2$ A_1	$l_{max}=2$ A_2	$l_{max}=2$ Normalized χ^2	$l_{max}=3$ A_1	$l_{max}=3$ A_2	$l_{max}=3$ A_3	$l_{max}=3$ Normalized χ^2
6.00	A	0.0117 ± 0.0017	−0.0412 ± 0.0015	15.5	0.0142 ± 0.0004	−0.0429 ± 0.0004	0.0041 ± 0.0003	1.0
5.97	P	0.0101 ± 0.0045	−0.0446 ± 0.0040	1.4	0.0120 ± 0.0085	−0.0466 ± 0.0083	0.0015 ± 0.0052	2.1
9.96	A	−0.0264 ± 0.0019	−0.0478 ± 0.0014	19.2	−0.0261 ± 0.0005	−0.0496 ± 0.0004	0.0045 ± 0.0003	1.1
9.87	P	−0.0203 ± 0.0037	−0.0479 ± 0.0025	1.2	−0.0192 ± 0.0029	−0.0528 ± 0.0028	0.0053 ± 0.0022	0.7
13.55	A	−0.0424 ± 0.0009	−0.0470 ± 0.0007	2.1	−0.0423 ± 0.0009	−0.0472 ± 0.0007	0.0007 ± 0.0006	2.1
13.55	P	−0.0352 ± 0.0040	−0.0456 ± 0.0034	1.3	−0.0355 ± 0.0045	−0.0450 ± 0.0042	−0.0011 ± 0.0036	1.6

B. Least-squares analysis

A least-squares analysis was made of the $A(\theta)$ data by fitting[8] the data to the expression[1]

$$k^2 \frac{d\sigma}{d\Omega} A(\theta) = \sum_{l=1}^{l_{max}} A_l(A) P_l^1(\cos\theta) \ . \qquad (2)$$

In the expression, $d\sigma/d\Omega$ is the unpolarized c.m. differential cross section, k is the magnitude of the c.m. wave vector in the initial channel, $P_l^1(\cos\theta)$ are the associated Legendre polynomials, and $A_l(A)$ are the expansion coefficients associated with the analyzing-power parameter. The values for $k^2(d\sigma/d\Omega)$ were obtained from the Legendre coefficients of McDaniels *et al.*[4] A linear interpolation was made between their coefficients at 13 and 14 MeV to obtain the coefficients at 13.55 MeV. Their coefficients at 6 and 10 MeV were used in fitting the 6.00- and 9.96-MeV data.

The normalized χ^2, defined as the χ^2 per degree of freedom (number of data points minus number of adjustable parameters) was used as the criterion for determining the goodness of fit to the data. The number of coefficients l_{max} was varied from one to five and a fit to the data was calculated for each value of l_{max}. We observed that in general the normalized χ^2 decreased as the number of parameters was increased from one to three but that no significant decrease was obtained for values of l_{max} greater than three. The results of this least-squares analysis of the data are presented in Table III. At 13.55 MeV the data are equally well fitted with $l_{max}=2$ or 3. At 6.00 and 9.96 MeV, however, there is unambiguous evidence for a $P_3^1(\cos\theta)$ term, whose significance will be discussed below.

A least-squares analysis was also made for neutron polarization data[9,10] at 5.97, 9.87, and 13.55 MeV. The data of Ref. 11 at 6.0 and 10.0 MeV, which disagree somewhat with those of Ref. 9, were rather arbitrarily not included in this analysis. The expression fitted is

$$k^2 \frac{d\sigma}{d\Omega} P(\theta) = \sum_{l=1}^{l_{max}} A_l(P) P_l^1(\cos\theta) \ , \qquad (3)$$

with the notation of Eq. (2). The resulting coefficients $A_l(P)$ are presented in Table III. At 6 MeV, $A_1(P)$ and $A_3(P)$ coefficients agree with those obtained by WM (Table A.1 of Ref. 2) from the analysis of other data. The $A_2(P)$ coefficients for both $l_{max}=2$ and $l_{max}=3$, however, disagree significantly with the corresponding experimental coefficients of WM. These disagreements reflect disparities in the different measurements of $P(\theta)$ (see Fig. 3). The normalized χ^2 of the present

analysis says that $l_{max}=2$ is adequate to describe the polarization data of Ref. 9.

C. Comparison of P and A

In Fig. 3 the angular distributions of P and A are compared at 6.0, 9.9, and 13.55 MeV. The analyzing powers are given by the squares which are as large or larger than the error bars assigned for these points. Polarization data are indicated by the open circles (Refs. 9 and 10)

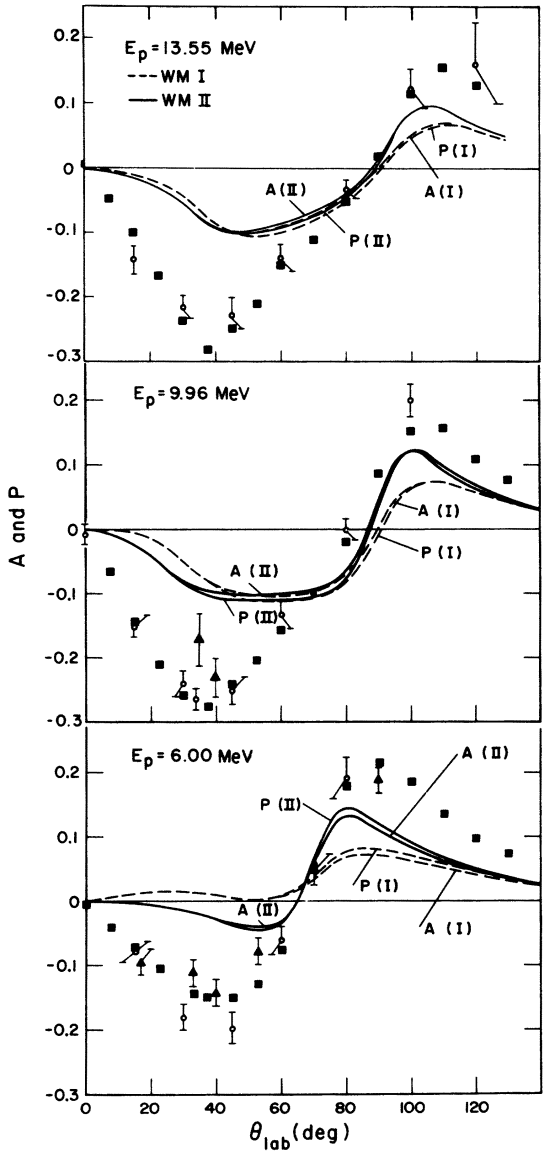

FIG. 3. $^3H(p,n)^3He$ analyzing power (squares) and polarization data from Refs. 9 and 10 (circles) and Ref. 11 (triangles). The broken lines indicate R-matrix calculations based on WMI and the solid lines indicate those based on WMII.

and triangles (Ref. 11). At 13.55 MeV the experimental A's and P's differ by more than 1 standard deviation only for the 15° (lab) point. At 9.9 MeV the 100° points disagree. The 35° polarization datum of Ref. 11 is also not consistent with either the polarization of Ref. 9 or the analyzing power. At 6 MeV there is some disagreement between the different polarization measurements but the average is not significantly different from the measured analyzing power. We conclude that at these energies there is no significant difference between the measured values of A and P.

Another quantitative comparison between P and A is in the associated Legendre-polynomial coefficients (Table III). For $l_{max}=2$, six pair of $A_l(A)$ and $A_l(P)$ can be compared. Of these only the A_1 coefficients at 9.8 and 13.55 MeV differ for P and A by more than one standard deviation. For $l_{max}=3$ there are nine pair. The A_1 coefficients at 9.9 and 13.55 MeV and the A_2 coefficients at 9.9 MeV differ by more than one standard deviation. These differences are expected statistically.

The present conclusion, therefore, is that at 6.0, 9.9, and 13.55 MeV there is no significant difference between the measured polarization and analyzing power of this reaction. In our previous work,[1] we compared A measured at $\theta_{c.m.}=45°$ with literature values of P from 1.5 to 12 MeV. At 6 MeV, the two observables were equal but, above 8 MeV, they appeared to disagree. The new polarization measurements[9,10] remove this disagreement at 9.9 and 13.55 MeV. The new data do not extend below 6 MeV, however. The large difference between P and A at $\theta_{c.m.}=45°$ between 1.7 and 4 MeV is still not understood.

D. R-matrix calculations

The observables P and A were calculated[12] with the two sets of R-matrix parameters of Werntz and Meyerhof.[2] The sets are designated[2] by WMI and WMII. The results are compared with the data in Fig. 3. The conclusions are similar to those of our previous studies of A at $\theta_{c.m.}=45°$ c.m. from 1.5 to 12 MeV,[1] of P at 13.55 MeV,[10] and of polarization transfer coefficients at 13.55 MeV[10] and at 0° from 3 to 16 MeV.[10,13] Namely, these sets of parameters account almost always for the signs but not the magnitudes of the various observables. The shapes of the angular distributions are also not very well described. On the other hand, these calculations do say that $P \cong A$ at least to within the accuracy of present polarization measurements. That result is in agreement with our conclusions at 6.0, 9.9, and 13.55 MeV.

E. Further considerations

The experimental results yield a simple relationship between two of the collision-matrix elements $U^{J}_{sl',sl}$ which are defined in the references of Ref. 2. The initial channel spin and orbital angular momentum are designated by s and l and they couple to total angular momentum J. The primed quantities refer to the exit channel. We restrict the quantum numbers as was done by WM, namely $l \leq 2$ and $J \leq 2$ and we neglect triplet d waves.

The associated Legendre-polynomial coefficient of the analyzing power $A_3(A)$ is given in terms of the collision-matrix elements by[1]

$$A_3(A) = \tfrac{1}{16}\,\mathrm{Im}(-3\sqrt{2}\; U^{2}_{0202}U^{1}_{0111}{}^{*}) \tag{4}$$

under the above restrictions on s, l and J. To the extent that these restrictions are valid, this simple combination of U matrix elements is given as $A_3(A)$ in Table III at 6.0, 9.9, and 13.55 MeV.

Further, less simple relationships that obtain if $P = A$ are given in the Appendix.

V. SUMMARY

We have measured angular distributions of the analyzing power $A(\theta)$ of the reaction $^3\mathrm{H}(\vec{p}, n)^3\mathrm{He}$ at 6.00, 9.96, and 13.55 MeV. The present results are not significantly different from the neutron polarization $P(\theta)$ at the same or nearby energies. The previous suggestion of a difference between P and A at the two higher energies has been resolved by new polarization data.

A fit of the angular distribution of $A(\theta)$ with associated Legendre polynomials shows the existence of a $P^1_3(\cos\theta)$ term at 6.00 and 9.96 MeV. This term is related to a simple expression of U^{2}_{0202} and U^{1}_{0111} if only angular momenta with $l \leq 2$, $J \leq 2$, and $s \neq 1$ if $l = 2$ are considered.

R-matrix calculations with the parameter sets of Werntz and Meyerhof confirm our previous conclusions that the signs of these analyzing powers, polarizations, and polarization transfer coefficients are reproduced, but quantitative agreement is lacking. The good precision of the present data emphasizes the disagreement.

ACKNOWLEDGMENTS

We wish to thank Dr. G. P. Lawrence and Dr. J. L. McKibben for providing the polarized-proton beam from the ion source, and Dr. R. L. Henkel and the tandem accelerator staff for their cooperation. One of us (JJJ) would like to thank the Associated Western Universities for financial support provided through the Associated Western Universities fellowship program.

APPENDIX

If $P \cong A$, the approximate equality may be expressed in relationships between the U matrix elements. For simplification the quantum numbers are restricted as in WM to $l \leq 2$ and $J \leq 2$ and triplet d waves are ignored. From the expressions[1] for $A_1(A)$ and $A_1(P)$:

$$\tfrac{1}{16}\,\mathrm{Im}(-3\sqrt{2}\,U^{1}_{1010}U^{1}_{1101}{}^{*} - 3\sqrt{2}\;U^{0}_{0000}U^{1}_{0111}{}^{*} + 3\sqrt{2}\;U^{2}_{0202}U^{1}_{0111}{}^{*}) \cong \tfrac{1}{16}\,\mathrm{Im}(-3\sqrt{2}\;U^{1}_{1010}U^{1}_{0111}{}^{*} - 3\sqrt{2}\;U^{0}_{0000}U^{1}_{1011} + 3\sqrt{2}\;U^{2}_{0202}U^{1}_{1011}{}^{*})\,. \tag{A1}$$

From the expressions for $A_2(A)$ and $A_2(P)$:

$$\tfrac{1}{16}\,\mathrm{Im}(-\tfrac{3}{2}\sqrt{2}\;U^{2}_{1111}U^{1}_{1101}{}^{*} - \tfrac{6}{2}\sqrt{2}\;U^{1}_{0101}U^{1}_{0111}{}^{*} - \tfrac{3}{2}\sqrt{2}\;U^{1}_{1111}U^{1}_{1101}{}^{*}) \cong \tfrac{1}{16}\,\mathrm{Im}(-\tfrac{3}{2}\sqrt{2}\;U^{2}_{1111}U^{1}_{0111}{}^{*} - \tfrac{6}{2}\sqrt{2}\;U^{1}_{0101}U^{1}_{1101}{}^{*} - \tfrac{3}{2}\sqrt{2}\,U^{1}_{1111}U^{1}_{0111}{}^{*}). \tag{A2}$$

And from $A_3(A)$ and $A_3(P)$

$$\tfrac{1}{16}\,\mathrm{Im}(-3\sqrt{2}\;U^{2}_{0202}U^{1}_{0111}{}^{*}) \cong \tfrac{1}{16}\,\mathrm{Im}(-3\sqrt{2}\;U^{2}_{0202}U^{1}_{1101}{}^{*}). \tag{A3}$$

These equalities hold to the extent that $A_l(A) = P_l(A)$ as indicated in Table III if the restrictions on l, s, and J are valid.

It should be noted that parameters derived from a charge-independent R-matrix analysis are not sufficient to guarantee these equalities or that $P = A$. Q-value effects and charge-dependent effects outside the channel radii break the symmetry between P and A.

*Work performed under the auspices of the U.S. Atomic Energy Commission.

†Associated Western Universities Fellow from the University of Wyoming, Laramie, Wyoming 82070.

‡Present address: Lawrence Livermore Laboratory, University of California, Livermore, California 94550.

§Visiting staff member to the Los Alamos Scientific Laboratory.

[1]R. C. Haight, J. J. Jarmer, J. E. Simmons, J. C. Martin, and T. R. Donoghue, Phys. Rev. Lett. 28, 1587 (1972).

[2]C. Werntz and W. E. Meyerhof, Nucl. Phys. A121, 38 (1968).

[3]L. Brown and U. Rohrer, private communication.

[4]D. K. McDaniels, M. Drosg, J. C. Hopkins, and J. D. Seagrave, Phys. Rev. C 6, 1593 (1972).

[5]G. P. Lawrence, G. G. Ohlsen, and J. L. McKibben, Phys. Lett. 28B, 594 (1969).

[6]G. G. Ohlsen, J. L. McKibben, G. P. Lawrence, P. W. Keaton, Jr., and D. D. Armstrong, Phys. Rev. Lett. 27, 599 (1971).

[7]Manufactured by Hamilton Watch Company, P.O. Box 1707, Lancaster, Pa. 17604

[8]R. H. Moore and R. K. Zeigler, Los Alamos Scientific Laboratory Report No. LA-2367, 1959 (unpublished). The least-squares fit to the data was made with the computer program PACKAGE. The program is described in the Los Alamos Scientific Laboratory Report No. LA-2367, 1959 (unpublished).

[9]J. J. Jarmer, R. C. Haight, J. C. Martin, and J. E. Simmons, to be published.

[10]R. C. Haight, J. E. Simmons, and T. R. Donoghue, Phys. Rev. C 5, 1826 (1972).

[11]R. L. Walter, W. Benenson, P. S. Dubbeldam, and T. H. May, Nucl. Phys. 30, 292 (1962).

[12]We are indebted to D. C. Dodder and G. M. Hale for assistance in performing these calculations.

[13]T. R. Donoghue, R. C. Haight, G. P. Lawrence, J. E. Simmons, D. C. Dodder, and G. M. Hale, Phys. Rev. Lett. 27, 947 (1971).